

## Supplemental Material

### **Label-free colorimetric logic gates based on free gold nanoparticles and the coordination strategy between cytosine and silver ions**

Yan Zhang <sup>a</sup>, Meng Li <sup>a</sup>, Haiyun Liu <sup>a</sup>, Shenguang Ge <sup>b</sup>, Jinghua Yu <sup>a,\*</sup>

<sup>a</sup> *School of Chemistry and Chemical Engineering, University of Jinan, Jinan 250022, P. R. China*

<sup>b</sup> *Shandong Provincial Key Laboratory of Preparation and Measurement of Building Materials, University of Jinan, Jinan 250022, P. R. China*

\*Corresponding to: Jinghua Yu

E-mail: [ujn.yujh@gmail.com](mailto:ujn.yujh@gmail.com)

Telephone: +86-531-82767161

Fax number: +86-531-82765969

## 1. Experimental

### 1.1. INHIBIT logic gate

An aqueous solution of S<sub>2</sub>-attached AuNPs solution was added into a tube. The INHIBIT<sup>1</sup> operation was triggered by four possible combinations of inputs: (1) H<sub>2</sub>O (0, 0); (2) 10 nM S<sub>1</sub> (1, 0); (3) 100 nM Ag<sup>+</sup> (0, 1); (4) 10 nM S<sub>1</sub> + 100 nM Ag<sup>+</sup> (1, 1).

### 1.2. Design and fabrication of simple PADs

The experimental detection results were obtained on simple PADs with a smartphone. The simple PADs were prepared similar to our previous work<sup>2</sup> with a modification and the detailed procedure was described below. Wax was employed as the paper hydrophobization and insulation agent to construct hydrophobic barrier on paper. As shown in Fig. S1, the sizes of the detection spots (paper sample zone) were with a diameter of 6 mm which were designed using Adobe illustrator CS4. The entire origami device could be produced in bulk on an A4 paper sheet by a commercially available solid-wax printer (Xerox Phaser 8560N color printer). Owing to the porous structure of paper, the melted wax could penetrate into the paper network to decrease the hydrophilicity of paper remarkably. After the curing process, the unprinted area (paper sample zone) still maintained good hydrophilicity, flexibility, and porous structure<sup>3</sup>.

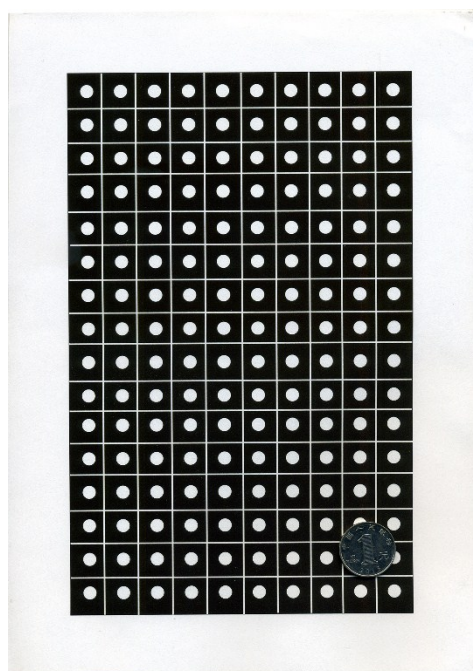


**Fig. S1** The schematic representation, size and shape of the simple PADs.

## 2. Results and Discussion

### 2.1. Optimization of experimental conditions

When varied concentrations of  $\text{Ag}^+$  were added to the prepared C-C mismatched  $\text{S}_1$ -attached AuNPs mixture, appreciable salt-induced colorimetric sensing could be observed. To achieve the optical colorimetric sensing, the effecting factors including pH value, and the response time were investigated as follows.

The pH value of the substrate solution was an important factor for colorimetric sensing. As shown in Fig. S2A, the optical response was achieved at pH 9.0 whether the  $A_{710}/A_{520}$  from UV-vis absorbance spectra or the blue/red ratio from the simple PDs. The response time was also an important parameter for the construction of colorimetric sensor. Fig. S2B showed the colorimetric results for  $\text{Ag}^+$  in centrifugal tube and on cellulose paper, respectively. The analytical blue/red color values of the spots for the AuNPs solution increased immediately following the addition of  $\text{Ag}^+$  and reached a plateau after 20 min. In contrast, the values in centrifugal tube samples kept rising even at an incubation time of 60 min. The fast response on simple PDs was attribute to that the paper device required a small amount of mixture (50  $\mu\text{L}$ ) and thus has a shorter diffusion length during color development. Consequently, the optimal conditions for various parameters were as follows: the pH value was 9.0, the response time was 20 min.

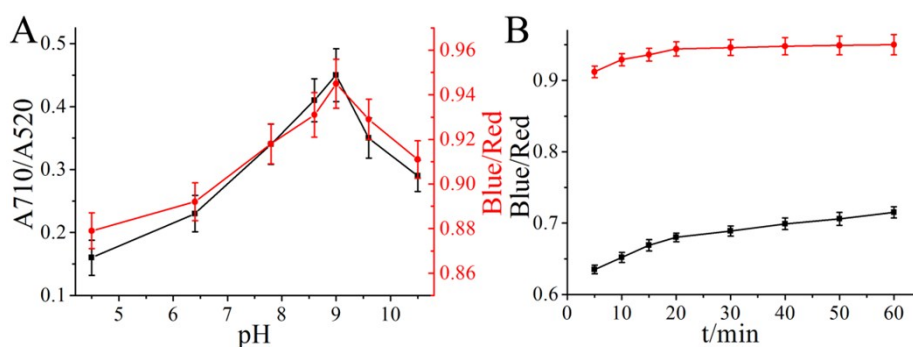


**Fig. S2** (A) Effects of pH value on (black)  $A_{710}/A_{520}$  values and (red) analytical blue/red color values of the spots; (B) Effects of incubation time on the colorimetric results (black) in centrifugal tube and (red) on cellulose paper in the presence of 100 nM  $\text{Ag}^+$ .

### 2.2. INHIBIT logic gate

The INHIBIT logic gate was represented by the situation where the output of an INHIBIT gate is true only if one input is true. By taking advantage of the disparate adsorption properties on AuNPs of ssDNA and dsDNA, an INHIBIT logic gate was

constructed with  $S_1$  and  $Ag^+$  as inputs (Fig. S3A). Fig. S3C showed the colorimetric results for the INHIBIT gate on cellulose paper. Little color change of  $S_2$ -attached-AuNPs mixture was obtained when  $Ag^+$  alone was added, while the color of  $S_2$ -attached-AuNPs mixture was changed from red to blue with the addition of  $S_1$ . The color change could be attributed to that the hybridization reaction could be performed with the addition of  $S_1$  to form dsDNA, which cannot prevent salt-induced AuNP aggregation. However, simultaneous addition of  $S_1$  and  $Ag^+$  significantly inhibited the dsDNA-induced aggregation of AuNPs solution, because the  $S_1$  and  $Ag^+$  were combined via C- $Ag^+$ -C coordination chemistry. In addition, the INHIBIT logic gate was also demonstrated by UV-Vis absorption spectra. A higher  $A_{710}/A_{520}$  value was obtained with  $S_1$  alone than with other combinations of the inputs (Fig. S3B). The results were in accordance with the truth table of the INHIBIT logic gate (Fig. S3D).

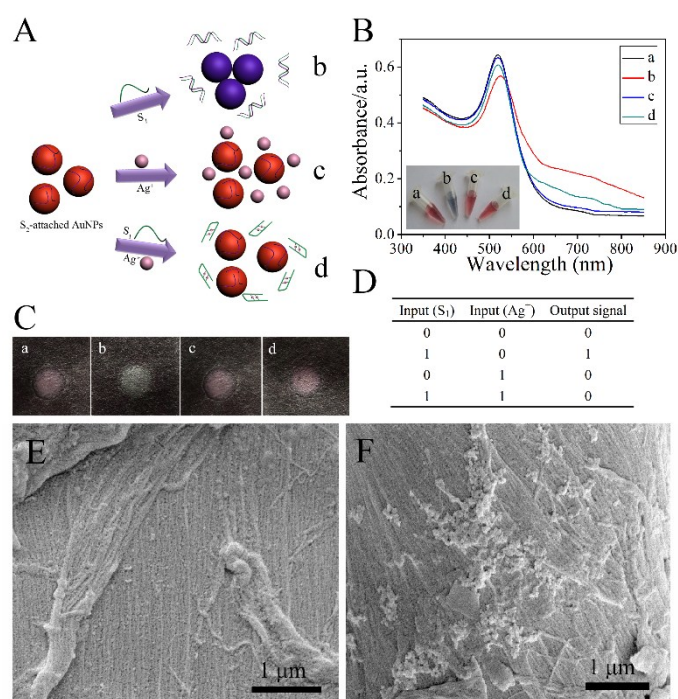


**Fig. S3** (A) Schematic representation of the INHIBIT logic gate:  $S_2$ -attached AuNPs solution treated with 10 nM  $S_1$  (b), 100 nM  $Ag^+$  (c), 10 nM  $S_1$  + 100 nM  $Ag^+$  (d). (B) UV-vis absorbance spectra of the INHIBIT logic gate:  $S_2$ -attached AuNPs solution without inputs (a),  $S_2$ -attached AuNPs solution treated with 10 nM  $S_1$  (b), 100 nM  $Ag^+$  (c), 10 nM  $S_1$  and 100 nM  $Ag^+$  (d), the inset was the photograph of AuNPs solution in corresponding condition. (C) The corresponding colorimetric sensing results of the INHIBIT logic gate on the simple PDs. (D) The truth table of the INHIBIT logic gate. SEM images of PAD treated with sample a (E) and sample b (F).

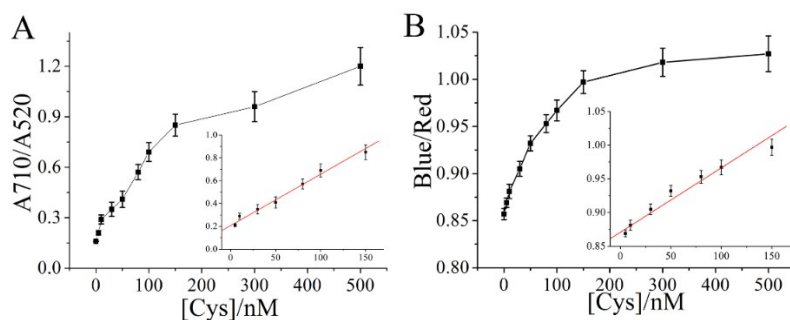


Fig. S4 Relationship between (A) A710/A520 values and (B) analytical blue/red color values of the spots and Cys concentration ( $n=5$ ), respectively. Inset: calibration curve of the (A) A710/A520 values and (B) analytical blue/red color values of the spots for Cys, respectively.

### 2.3. Selectivity of the colorimetric assay for Cys

For an excellent assay, high specificity is a matter of necessity. To study the selectivity of the sensing system for Cys determination with current approach, the degrees of color variance of mixture spots containing various amino acids found in proteins (1000 nM) were obtained and compared with that of Cys (100 nM). Fig. S5 showed the experimental results, and it was clearly that three aminothiols (Cys, Hcy, and GSH) could induce the color change of blue, whereas no obvious color change was observed by other amino acids even at high concentrations. Which was attributed to the similar characteristic of the three aminothiols.<sup>4,5</sup> This result indicated that the method could also be expanded to assay other thiol-containing biomolecules, such as the non-proteinogenic amino acid of homocysteine, the small peptide of glutathione.

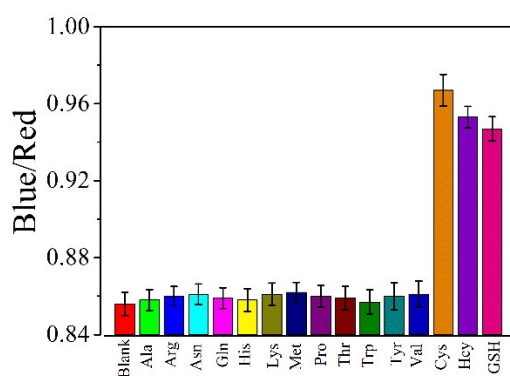


Fig. S5 Specificity test results obtained for samples of the analytical blue/red color values obtained using the proposed sensing platform. The concentrations for Cys and other amino acids are 100 nM, and 1  $\mu$ M, respectively.

### References

1. Z. Z. Huang, H. N. Wang and W. S. Yang, *Nanoscale*, 2014, **6**, 8300.
2. M. Li, Y. H. Wang, Y. Zhang, J. H. Yu, S. G. Ge, M. Yan, *Biosens. Bioelectron.*,

2014, **59**, 307.

3. E. Carrilho, A. W. Martinez, G. M. Whitesides, *Anal. Chem.*, 2009, **81**, 7091.
4. Y. Lin, Y. Tao, F. Pu, J. Ren, X. Qu. *Adv. Funct. Mater.*, 2011, 21, 4565.
5. Zhang, B. Lu, C. Lu. *Analyst*, 2013, 138, 850.